

# Hydration Sphere Structure of Proteins: a Theoretical Study

Anikó Lábás<sup>1</sup>, Imre Bakó<sup>2\*</sup> and Julianna Oláh<sup>1\*</sup>

<sup>1</sup> Department of Inorganic and Analytical Chemistry, Budapest University of Technology and Economics, Szent Gellért tér 4, H-1111 Budapest, Hungary

<sup>2</sup> Institute of Organic Chemistry Research Centre for Natural Sciences, Hungarian Academy of Sciences Magyar tudósok körútja 2. H-1519 Budapest, P.O. Box 286, Hungary

1  
2  
3  
4  
5  
6  
7  
8  
9

---

\* corresponding author, to whom corresponding should be addressed

e-mail: [julianna.olah@mail.bme.hu](mailto:julianna.olah@mail.bme.hu); telephone number: +36-1-463-1286

e-mail: [bako.imre@ttk.mta.hu](mailto:bako.imre@ttk.mta.hu); telephone number: +36-1-382-69-81

10 **Abstract**

11 Hydration is essential for the proper biological activity of biomolecules. We studied the water  
12 network around insulin (as a model protein) in aqueous NaCl solutions using molecular dynamics  
13 simulations and statistical analysis of the topological properties (hydrogen bond neighbor number  
14 and the interaction energy between hydrogen-bonded water molecules) of the water network. We  
15 propose a simple method to define the hydration layers around proteins. Water molecules in the first  
16 and second layers form significantly less, but stronger hydrogen bonds with each other than in the  
17 bulk phase. Furthermore, water molecules over the hydrophilic and hydrophobic surface of the  
18 protein possess slightly different H-bonding properties, supporting the hypothesis of structural and  
19 dynamical heterogeneity of the water molecules over protein surface. The protein molecule perturbs  
20 the solvent structure at least up to the fourth-fifth hydration layer. Our data suggest the peculiar role  
21 of the second hydration shell.

22

23

24

25 **Keywords:** hydrogen-bond network, hydration sphere, MD simulations

## 26 **Introduction**

27 The appropriate spatial structure is essential for the activity of proteins. It is affected by both  
28 intramolecular interactions in the proteins and the intermolecular interactions formed with the  
29 solvent molecules, which is water in living cells. It has been well-established that the dominant  
30 conformational motions of proteins are profoundly affected by their hydration shell.[1,2] As a  
31 consequence, structural changes of the solvent should inevitably affect protein structure and function  
32 as well. Indeed, addition of compounds such as inorganic salts, organic molecules, acids or bases to  
33 the solution can perturb the structure of liquid water leading to the denaturation of the biomolecule.  
34 Among these, the denaturing effect of salts has been the most extensively studied, and more than a  
35 century ago Franz Hofmeister ordered the ions according to their ability to precipitate egg-white  
36 proteins.[3,4] Kosmotropic ions (e.g. sulfate ion) or water structure makers strengthen the hydrogen-  
37 bonding network of bulk water and at the same time decrease the solubility of biomolecules. In  
38 contrast chaotropic ions (e.g. nitrate ion) supposedly break the hydrogen-bonding network of bulk  
39 water and increase the solubility of biomolecules. Recently, the interfacial tension at the  
40 protein–water interface was shown to play a central role in the Hofmeister phenomena.[5] Not only  
41 salts, but other chemical agents can also denature proteins. Bennion and Daggett simulated the urea-  
42 induced denaturation of chymotrypsin and suggested that the solvent plays various roles in the  
43 process. Most importantly, the structure and dynamics of the solvent changed in the solution, and  
44 intrusion of the solvent molecules into the hydrophobic core of chymotrypsin was responsible for  
45 diminishing the hydrophobic effect and encouraging solvation of the core and thereby changing the  
46 intramolecular hydrogen bond network in the protein.[6]

47 Generally, it is accepted that different levels of hydration occur at a biomolecule. In the first  
48 hydration layer water interacts with the external surface of the protein through directional hydrogen-  
49 bonding (H-bonding) interaction especially on the hydrophilic surface of the protein, while on the  
50 hydrophobic surface of the protein the topology, roughness and spatial constrains of the surface  
51 orient the water molecules. As a consequence, the hydrogen-bonded properties of water is influenced  
52 significantly by the surface properties of macromolecules resulting in increased mean residence  
53 time[7–12] and 10-20% increase of the density of water molecules[13,14] compared to the bulk  
54 phase. However, a molecular dynamics study on myoglobin, also showed that only those water  
55 molecules have very long residence times that are found in cavities and clefts of the protein; other  
56 hydration sites of the protein are characterized by residence times similar to the bulk phase.[15] The  
57 water-water hydrogen bonding in the first layer forms a spanning, peptide homogeneously  
58 enveloped, percolated network, while lack of biological functions is always connected to the broken

59 (not percolated) H-bonded network in the first layer.[16] Recent terahertz spectroscopic  
60 measurements, a method sensitive to the collective motion of water molecules, indicate that protein  
61 disturb the water structure beyond the 1-2 water layers as previously thought.[17] The radius of the  
62 dynamic hydration shell was greater than 10 Å for the studied proteins and correlated well with the  
63 dipole moment of the protein.[18]

64 It is obvious from the above overview that gaining a better understanding of the hydration layer  
65 structure around proteins could contribute to our understanding of various processes involving  
66 protein-solvent interactions such as protein folding and unfolding. A possible way to study the  
67 structure of water is graph theory, which has recently been applied to the hydrogen bond network in  
68 various solutions and mixtures, e.g. of water, methanol and ethanol solutions adsorbed in  
69 microporous silicalite-1[19], of ion aggregates in different high salt solutions[20], and of highly  
70 concentrated renal osmolyte solutions.[21] Recently, we studied the mixtures of water and  
71 formamide, the simplest model of the peptide bond, and showed that these two compounds form  
72 microhomogeneous mixtures, in which the number of hydrogen bonds formed by water and  
73 formamide are very similar.[22]

74 When graph theory is used to study the structure (i.e. hydrogen bond network) of water, the network  
75 of interactions is mapped into a graph.[23] The vertices of the graph correspond to the water  
76 molecules and the edges to the hydrogen bonds formed by the water molecules. Once the hydrogen  
77 bond network is mapped into a graph, a thorough statistical analysis can be carried out in order to  
78 get insight into the water structure.

79 In the present work we extend this theory to explore the hydrogen bond network around a protein to  
80 obtain a better understanding of its structure and how it changes from the surface of the protein  
81 towards the bulk phase, and investigate how molecular dynamics simulations can give more insight  
82 into recent findings by terahertz spectroscopic measurements that proteins disturb the water structure  
83 beyond 1-2 water layers. Furthermore, we explore the effect of salt concentration on the properties  
84 of the hydrogen bond network around a protein. We chose insulin as a model protein because of its  
85 (1) small size (2) importance in human health (3) and as it has a balanced distribution of hydrophobic  
86 and hydrophilic patches on its surface. NaCl was selected as a co-solute to the protein, because Na<sup>+</sup>  
87 has a relatively high concentration in the cytosole compared to divalent cations and it has a weak  
88 hydrate sphere ordering capacity and Cl<sup>-</sup> is by far the most common anion in living organisms.

89 First we carried out a series of molecular dynamics simulations at different salt concentrations on  
90 solvated systems (with and without the protein), then for each snapshot taken from the trajectory of

91 the simulations, we determined the network of hydrogen bonds and transformed it to a graph. Finally,  
92 a thorough statistical analysis of the properties of the obtained graphs (hydrogen bond neighbor  
93 number and the interaction energy between hydrogen-bonded water molecules) were carried out.  
94 Importantly, we present here a simpler approach to define solvent layers around the protein compared  
95 to those that have been described in the literature,[24–26] and investigate their hydrogen bond  
96 properties layer by layer, which enables us to compare the structure and hydrogen bond properties  
97 of these layers to those of reference solutions, which do not include the protein molecule. This  
98 methodology enables us to characterize the effect of the protein molecule on the hydrogen bond  
99 network and to study the structure of its hydration sphere in a statistical way.

## 100 **Methods**

101 **Molecular dynamics simulations (MD).** The crystal structure of the monomer, which is the active  
102 form of human insulin (PDB code 3I40[27]) was used as a starting structure for the MD simulations.  
103 Disulfide bonds were created between Cys<sub>6,chainA</sub>-Cys<sub>11,chainA</sub>, Cys<sub>7,chainA</sub>-Cys<sub>7,chainB</sub> and Cys<sub>20,chainA</sub>-  
104 Cys<sub>19,chainB</sub>. The protonation state of the titratable amino acid residues were determined using the  
105 H++ webserver version 3.2.[28–30] Based on the estimated pK<sub>a</sub> values the His<sub>5</sub> residue was doubly  
106 protonated in chain B and after visual analysis of their surroundings all other histidine residues were  
107 protonated on the ε nitrogen atom. The CHARMM-GUI webserver was used for the system setups  
108 and generation of the input files.[31], the NAMD software package[32] with the CHARMM27 force  
109 field[33] for the minimization of the structure and dynamics simulations. Hydrogen atoms were  
110 added using the standard CHARMM protocol.[34] We chose the TIP3P water model, which is a  
111 simple 3-point rigid water model, to simulate water as the non-bonded parameters of protein atom  
112 types in the CHARMM27 force field were determined to be in line with the TIP3P water model. As  
113 a consequence, when the CHARMM program package is used for modelling proteins the TIP3P  
114 water model is by far the most frequently used water model, yielding a reliable description of  
115 proteins. Therefore, the protein was solvated by TIP3P water molecules arranged in an octahedral  
116 shape with 15 Å edge distances. Three differently solvated protein systems were prepared. One  
117 contained only one sodium ion in order to generate a neutral system, while two other systems  
118 contained sodium and chloride ions in 0.5 and 1.5 molar concentrations. Although the cytosolic  
119 concentration of these ions is much lower, we have chosen these relatively high concentrations to  
120 obtain improved statistics for the effect of the desalting in the simulation. The ions were placed by a  
121 Monte Carlo approach. Reference systems of the salt solutions with 0 M, 0.5 M and 1.5 M  
122 concentrations were also prepared; these did not include the protein molecule. Afterwards, each  
123 system was minimized for 10000 steps to eliminate bad initial contacts, followed by a 50 ps long  
124 NVT equilibration simulations at 303.15 K temperature. Then 5 ns long NPT Langevin MD  
125 simulations were carried out applying 2 fs step size with collecting configurations from every ps. All  
126 bonds in the molecules involving hydrogen atoms were kept fixed with the SHAKE[35] algorithm.  
127 Periodic boundary conditions (PBC) were used to handle boundary effects. The temperature was set  
128 to 303.15 °C in all simulations. The equilibration of the systems was reached by means of  
129 temperature reassignment. All of the velocities of the atoms in the systems were periodically  
130 reassigned in order to set the desired temperature. Therefore, in every 500 steps the temperature was  
131 rescaled during equilibration. The Constant Temperature Control making use of Langevin dynamics.  
132 was applied together with the Nose-Hoover Langevin piston pressure control with the target pressure

133 set to 1.01325 bar. As the random initial velocity distribution used in the MD simulation could  
134 influence the obtained results, all MD simulations were carried out with three different initial  
135 velocity distributions yielding 3-3 parallel trajectories for all systems studied.

## 136 Analysis

137 **Hydrogen bonds.** Two water molecules were regarded hydrogen bonded if the H $\cdots$ O distance  
138 between the two molecules was smaller than 2.5 Å and O-H $\cdots$ O angle was larger than 120°. This  
139 criteria are reasonable for protein simulations where correlation between the distance and the angle  
140 criteria have already been shown.[36] However, we have checked the dependency of our results on  
141 this definition by analyzing the trajectories obtained for the protein solvated in 0.5 M NaCl solution  
142 by setting the O-H $\cdots$ O angle criterion to 130° and 145° as well.

143 The average hydrogen bond number,  $N_{\text{HB}}$ , was calculated by averaging the number of hydrogen  
144 bonds over the trajectory and over all molecules (Eq. 1):

$$N_{\text{HB}} = \frac{\langle \sum_{i=1}^N N_{\text{HB},i} \rangle}{2N} \quad (1)$$

145 where  $N_{\text{HB},i}$  is the number of hydrogen bonds around water molecule  $i$ ,  $N$  is the number of water  
146 molecules in the simulated box and  $\langle \rangle$  denotes averaging over all snapshots.

147 We calculated the hydrogen bond energy between water molecules  $i$  and  $j$  ( $E_{\text{HB},ij}$ ) for each hydrogen  
148 bond using the TIP3P force field following the common practice[37] to identify the hydrogen-bond  
149 energy with the interaction energy of the H-bonded molecular pair, even if the H-bond energy cannot  
150 be separated from the rest of the pair interaction energy. It was averaged over all hydrogen bonded  
151 pairs and over the whole length of the trajectory to yield the average hydrogen bond energy ( $E_{\text{HB}}$ )  
152 using the following equation:

$$E_{\text{HB}} = \frac{\langle \sum_{i=1}^N \sum_{j=1}^{N_{\text{HB},i}} E_{\text{HB},ij} \rangle}{\langle \sum_{i=1}^N N_{\text{HB},i} \rangle} \quad (2)$$

153  $E_{\text{HB},ij}$  is the energy of the hydrogen bond between molecules  $i$  and  $j$  and the rest of the notation  
154 corresponds to Eq. 1.

155

156 **Definition of solvation layers.** As experimental data indicate that proteins disturb considerably the  
157 water structure around them, we have developed a methodology to define hydration layers around  
158 the protein (**Fig. 1**). Molecules on the surface of the protein (first layer) were defined according to  
159 two rules: **(1)** water molecules were assigned to interact with the hydrophilic surface of the protein

160 if any of the following distances ( $O_{\text{Water}}-H_{\text{Protein}}$  or  $H_{\text{Water}}-O_{\text{Protein}}$  or  $H_{\text{Water}}-N/S_{\text{Protein}}$ ) was smaller than  
161 2.5 Å and (2) water molecules in the first layer interacting with the hydrophobic surface of the protein  
162 were defined as having a  $C_{\text{Protein}}-O_{\text{Water}}$  (abbreviated to C-O distance from now on) distance smaller  
163 than 4.5 Å and not satisfying rule (1). Application of these two rules provided us with a continuous  
164 first hydration layer over the surface of the protein. The second hydration layer consisted of the water  
165 molecules having an  $O_{\text{Water}}-O_{\text{Water,layer (1)}}$  distance smaller than 3.5 Å and not belonging to layer (1).  
166 From this on water molecules were assigned to belong to layer n+1 having an  $O_{\text{Water,layer(n+1)}}-O_{\text{Water,layer(n)}}$   
167 distance smaller than 3.5 Å and not belong to layer n. 4.5 Å was chosen as the critical  
168 C-O distance, because it is very close to the minimum of the partial radial distribution function of  
169 the C-O distance in liquid methanol or of the C- $O_{\text{water}}$  distance in water-methanol mixtures. It is also  
170 the typical C-O distance between the carbon atom of CH<sub>3</sub> groups and the oxygen atom of the water  
171 molecule closest to them. However, we have tested the dependency of our results on this distance,  
172 and the analyses were performed using 4.0, 4.25, 4.5 and 5 Å criteria as well in the case of insulin  
173 system solvated in 0.5 M NaCl solution.

174

## 175 Results

176 **Protein behaviour at different salt concentrations.** We compared the behavior of the proteins at  
177 various salt concentrations in the MD simulations. The results have been averaged over all snapshots  
178 of the productive part of the MD simulation and over the three parallel trajectories carried out at  
179 identical salt concentrations. In order to check the stability of the protein conformation during the  
180 simulations we have calculated the Root Mean Square Deviation (RMSD) of the atomic positions.

$$RMSD = \sqrt{\frac{\sum_{i=1}^N (r_i(t_1) - r_i(t_2))^2}{N}} \quad (3)$$

181 where N is the number of atoms and  $r_i(t)$  is the position of atom i at time t. In all cases  $t_1$  was the  
182 position of the protein heavy atoms after the heating up of the system. The comparison of the protein  
183 RMSD values for all trajectories is shown in **Table 1**, decomposed according to the various structural  
184 elements found in insulin. The structural elements are shown in **Fig. 2**. While the obtained RMSD  
185 values are similar in the cases of the neutralized and 0.5M NaCl systems, slightly lower RMSD  
186 values have been observed in the case of the 1.5M NaCl system. This could originate from the fact  
187 that in this reasonably concentrated 1.5M solution ions have a stronger tendency to absorb on the  
188 surface of the protein and slightly stabilize its structure as the ion-surface interaction is much stronger  
189 than the H-bonds between the surface and the water molecules.



190 The RMSD values show that insulin remained in its natural conformation along the MD trajectory.  
191 We were also interested to check how other parameters, the radius of gyration and the geometric  
192 moment tensor changed along the trajectory, as they could also give insight into structural changes  
193 of the protein. Nayar et al showed that the gyration radius of a globular protein (of the 16-residue  
194  $\beta$ -hairpin fragment of the 2GB1 protein) shows a remarkable (at least 1.5-2 Å) difference between  
195 its folded and unfolded states.[38] The gyration radius of insulin ( $10.1 \text{ \AA} \pm 0.1 \text{ \AA}$ ) was quite stable  
196 during the whole simulation in all three solution. indicating the stability of the protein structure.

197 Globular proteins in their native conformation, like insulin, have close-packed structures with quite  
198 high number densities and a well-defined shape in the solution. Characterization of the shape of  
199 proteins has been in the focus of intense scientific interest for many years. One of the applicable  
200 method for the description of the shape of a whole protein uses simple ellipsoids. Here, we apply for  
201 this purpose the size of the three main axes of the geometry moment tensor, which is calculated with  
202 a similar mathematical construction, as the moment of the inertia tensor, with the difference that each  
203 point (i.e. the coordinates of all heavy atoms) is assigned the same mass: a mass of unity, instead of  
204 the real mass of the atom. The values of the size of the three main geometrical moments as a function  
205 of time are presented in **Fig. 3** in the case of the 1.5 M solution, but we obtained very similar graphs  
206 in the case of the other two concentrations as well. The figure shows that that the overall shape of  
207 the protein does not change significantly during the simulation time. This method also enables us to  
208 characterize the shape of the solvation layers. We performed this for this first three hydration layers  
209 together, which is also shown in **Fig. 3**. It is obvious that the shape of the solvation layers closely  
210 follow that of the protein, with longer axes.

211 **Number of the water molecules in the solvation layers.** We determined the number of water  
212 molecules in each shell around the protein (see **Table 2**). As expected as a function of layer number  
213 the number of water molecules increases significantly at each salt concentration as we go farther  
214 away from the protein. It seems that there is no significant difference between the number of water  
215 molecules in the first and second shell around the protein in the case of the neutralized system and  
216 the 0.5 M NaCl concentration system, while there seem to be less water molecules around  
217 hydrophilic surface of the protein in the simulations with the highest salt concentration. Here it is  
218 worth noting, that  $\text{Na}^+$  and  $\text{Cl}^-$  are neither chaotropic nor kosmotropic, thus they have no strong  
219 tendency either to be attracted nor to be repelled from the surface of proteins. We examined the  
220 number of water molecules associated to the hydrophilic and hydrophobic surface of the protein and  
221 it is seen that at all concentrations the number of water molecules at the hydrophobic surface remains  
222 identical, but decreases slightly at the hydrophilic surface. There are most likely two different reasons

223 for this: (1) the solvent accessible surface area of the protein slightly decreases and as such fewer  
224 water molecules can access it (2) with increasing salt concentration, the “place” of several water  
225 molecules is taken over by ions, which can also occur especially on the hydrophilic surface of the  
226 protein. This finding is in accordance with the expectation that ions are repelled from  
227 hydrophobic/non-polar regions. As we go farther away from the protein surface we find an increasing  
228 difference among the number of molecules in a given shell with increasing salt concentration due to  
229 the presence of an increasing number of ions.

230 **Radial distribution function.** The oxygen-oxygen ( $O_{\text{water}}-O_{\text{water}}$ ) partial radial distribution function  
231 (RDF) can be used for characterization of the structure of water around the protein surface.[39,40]  
232 We calculated two different types of radial distribution functions to evaluate the extent of the water  
233 structure around protein surface. In one of them we calculated the RDF for the interactions between  
234 the water molecules in the first layer- and all other water molecules in layers 2-4 to obtain the surface  
235 distribution function (SDF). In the other case water-water RDF was calculated only for water  
236 molecules in the first layer. Unfortunately, from our simulations we do not know a priori the exact  
237 density of water in the simulation box and we could not properly calculate the excluded volume  
238 effect, so the raw  $O_{\text{water}}-O_{\text{water}}$  density distribution was determined using the spherical average  
239 method according to Eq. 4.:

$$\rho(r) = \frac{N(r)}{(4\pi r^2 dr)} \quad (4)$$

240 where N denotes the number of particles. It can be seen from both **Figs. 4** and **5** that the curvature of  
241 the raw density distribution functions is the same for all interaction types, thus we can assume that  
242 the necessary corrections to account for the excluded volume effect would be the same in all cases,  
243 thus we can obtain correct trends from the raw distribution functions as well.

244 In **Fig. 4** the surface distribution functions are shown for the interactions between hydrophobic- and  
245 hydrophilic-all other water molecules in layers 2-4 cases. We cannot detect any large changes on  
246 these SDFs as a function of salt concentration. The first peak on these SDF is around 2.8 Å and it is  
247 significantly more pronounced for the hydrophobic surface water-all water case.

248 The raw density distribution functions corresponding to the first layer-first layer structure are  
249 presented in **Fig. 5**. On the inset we presented the long range behavior of these functions, which  
250 show that the long range behavior of these function is the same for different interaction types:  
251 hydrophilic-hydrophilic (Hy-Hy), hydrophobic-hydrophobic (Hyb-Hyb) and hydrophilic-  
252 hydrophobic (Hy-Hyb); thus these functions can be compared. The H-bonded structure, which can

253 be characterized by the first peak at around 2.8 Å is more pronounced in the Hyb-Hyb case, which  
254 is in good agreement with results of statistical analysis of H-bond strength (see below). The shape  
255 of the first peak of the hydrophilic-hydrophilic (Hy-Hy) RDF is considerably deviates from the other  
256 two (Hyb-Hyb,Hy-Hyb) RDFs, especially in the range of 3.2-4.5 Å. This difference in shape  
257 indicates (1) the uniformity of the interaction between water molecules over the hydrophobic surface  
258 of the water molecules (2) larger differences in interaction strengths between water molecules over  
259 the hydrophilic surface of the water. This implies that water molecules behave differently over the  
260 hydrophobic and hydrophilic surface of the protein and supports the hypothesis of structural and  
261 dynamical heterogeneity of the surface.

262 **Average hydrogen bond number.** Next, we determined the average number of hydrogen bonds  
263 formed by water molecules in the reference aqueous solutions not including the protein, then we  
264 analyzed the hydrogen bonds formed by water molecules in the protein-containing systems. In the  
265 latter case we determined how many hydrogen bonds are formed between water molecules in the  
266 same layer, and between two layers as well. In the case of the first hydration layer the data was even  
267 further decomposed that we could see the effect of the protein on the hydrogen bond network. The  
268 data is collected in **Table 3**. In the reference solutions, the average hydrogen bond number in the  
269 pure water and at 0.5 M NaCl solution is 3.4 which agrees very well with the results of earlier  
270 studies.[23,41] At the highest salt solution, the average hydrogen bond number is decreased to 3.14,  
271 which clearly originates from the fact that at such a high salt concentration, significant number of  
272 hydrogen bonding sites of the water molecules are occupied by the solute ions, *i.e. the water*  
273 *molecule itself belongs with an increasing probability to the solvent sphere of an ion.*

274 Water molecules in the 1<sup>st</sup> solvation shell establish significantly lower number of hydrogen bonds  
275 with other water molecules than in the bulk phase (e.g.  $n_{\text{HB,ref}}=3.40$  at 0.5M), but this effect is  
276 *overcompensated* by the hydrogen bonds established with the protein. In the 2<sup>nd</sup> shell significantly  
277 smaller number of hydrogen bonds are found compared to the bulk phase or the other solvation  
278 layers. From the 3<sup>rd</sup> shell the average hydrogen bond number and the structure of the hydrogen bond  
279 network begins to resemble to the reference systems, although the total number of hydrogen bonds  
280 is slightly larger. As a result of the increase of the salt concentration the number of the hydrogen  
281 bonds ( $N_{\text{HB}}$ ) decreases, and water molecules in the 3<sup>rd</sup> and 4<sup>th</sup> solvation shells form similar number  
282 of hydrogen bonds than found in the reference systems (aqueous solutions with identical salt  
283 concentration). (Here we would like to note that in the reference systems the hydrogen bonds among  
284 water molecules that are not in the coordination sphere of sodium or chloride ions are stronger by  
285 *1.7- 2.5 kJ/mol* than the average hydrogen bond number averaged over all water molecules.) Our

286 data show that the number of hydrogen bonds in the 1<sup>st</sup> solvation shell are considerably larger than  
287 in the 2<sup>nd</sup> layer. The number of hydrogen bonds ( $N_{HB}$ ) formed only within the 1<sup>st</sup> shell is around 1.8  
288 and the occurrence of a few very large clusters in the cluster size distribution indicate the formation  
289 of a percolated network (i.e. a continuous network of interconnected clusters) in good agreement  
290 with previous data of Brovchenko et al.[42] We performed the same cluster analysis for solvation  
291 layers 2, 3 and 4 separately, taking into account only the in-layer H-bonds, but in these layers the  
292 water molecules do not form a percolated network in any of these layers. The average number of  
293 hydrogen bonds formed among water molecules in the 2<sup>nd</sup> solvation shell is remarkably small. This  
294 is due to the fact that while water molecules in the 1<sup>st</sup> layer orient themselves to form as many  
295 hydrogen bonds with the protein as possible, the 3<sup>rd</sup> layer orients itself towards bulk water, but water  
296 molecules in the 2<sup>nd</sup> layer cannot easily accommodate themselves to establish an optimal number of  
297 hydrogen bonds. This is best regarded as a transient layer whose properties are determined by a  
298 combined effect of the adaptation to the shape of the protein molecule and to the network of water  
299 molecules in the bulk solvent.

300 We have checked the dependence of the results on the applied H-bond criteria. In **Table 4** we have  
301 collected the data obtained with various C-O distances used to allocate water molecules over the  
302 hydrophobic surface of the protein. It can be observed that the C-O distance primarily influences the  
303 average H-bond neighbor number in the first shell, taking longer distance the  $n_{HB}$  slightly increases.  
304 The same effect is observed in the second shell although to a lesser extent, but no effect can be seen  
305 in the case of the farther layers. The reason observed for the first two layers arises from the fact that  
306 by changing the C-O distance the number of water molecules slightly changes over the hydrophobic  
307 surface of the protein, some molecules may be assigned to layer 1 or layer 2 depending on the exact  
308 C-O distance, but at larger distances this effect diminishes. However, it is important to emphasize  
309 that our conclusions do not depend on the exact value of the C-O distance between 4-5 Å.

310 We have also investigated how the obtained results depend on the angle criteria used to determine  
311 hydrogen bonds. The data in **Table 5** show that with using a larger angle criterion, the average H-  
312 bond neighbor number slightly decreases as only more “perfect” H-bonds are identified as H-bonds  
313 (i.e. a smaller number of them is found), but the observed trends do not change at all.

314 **Changes in hydrogen bond energy as a function of the distance from the surface of the protein.**  
315 For the characterization of the hydrogen bonded interaction we can use the strength of the hydrogen  
316 bond. This strength is identified by the interaction energy of the two hydrogen bonded water  
317 molecules. In order to sign the perturbation effect of the protein we have investigated the average  
318 hydrogen bond energies in each layer and between the layers. Student's t-test, a rigorous statistical

319 probe, was used to prove that the observed differences between the obtained values are significant.  
320 Data in **Table 6** show that the strongest hydrogen bonds between water molecules are formed in the  
321 pure liquid water reference system, and addition of solutes (either protein or salt) decreases the  
322 hydrogen bond strength, and this decrease becomes more significant with increasing salt  
323 concentration. Furthermore, **Table 7** shows that changing the angle criteria does not influence the  
324 observed trends. We can decompose this value to calculate the hydrogen bond energy strength  
325 between water molecules associated to the hydrophilic or to the hydrophobic surface of the protein.  
326 It is clear from these data that hydrogen bonds among water molecules at the hydrophobic surface  
327 are much stronger than at the hydrophilic surface. This is due to the protein-water interactions at the  
328 hydrophilic surface, where water molecules orient themselves to interact mainly with protein surface  
329 groups. However, over the hydrophobic surface water molecules mainly interact with each other  
330 leading to more optimal hydrogen bonded arrangements. Furthermore, the average hydrogen bond  
331 strength in the first layer is mainly governed by interactions of the hydrophobic water molecules,  
332 and suggests that the interaction between a hydrophobic and hydrophilic water molecule is also very  
333 strong. These results are in a good agreement with the differences of the water-water partial radial  
334 distribution functions calculated for the various parts (hydrophobic or hydrophilic) of the protein  
335 surface (**Fig. 5**).

336 We also observe considerable difference in the strength of the interactions between and in the layers  
337 (e.g. in the case of the 0.5M system: inside the 2<sup>nd</sup> layer -14.88 kJ/mol and between the 2<sup>nd</sup> and 3<sup>rd</sup>  
338 layers -15.34 kJ/mol, respectively), which indicates that the perturbation effect caused by the protein  
339 shape is more pronounced in interactions in the layers than between the layers. This phenomenon is  
340 in the 4<sup>th</sup> and 5<sup>th</sup> layers begin to disappear. In these layers the strength of the hydrogen bonds is  
341 getting closer and closer to the values observed in the reference systems. (Here we would like to note  
342 that in the reference systems the hydrogen bond strength between water molecules that are not in the  
343 coordination sphere of sodium or chloride ions is only 0.08-0.13 kJ/mol stronger than the average  
344 hydrogen bond strength averaged over all water molecules.) Due to the salt concentration, the  
345 average hydrogen bond strength decreases in the same way as in the reference systems.

#### 346 **Relevance of our results to physiological solutions**

347 After having examined numerous properties of the hydrogen bond network around insulin, used as  
348 a model protein, it is worth putting our results into a wider context and consider their relevance to  
349 physiological and other solutions. The data show that proteins disturb the H-bond network at least  
350 up to five water layers, which imply a large volume of water and reasonably large distances between  
351 the protein molecules. We calculated the concentration of the protein in our systems to be  $8.360 \cdot 10^{-}$

352  $^3$  M,  $8.762 \cdot 10^{-3}$  M and  $9.595 \cdot 10^{-3}$  M in the neutral, 0.5 M and 1.5M NaCl solutions, respectively.  
353 As an example of a physiologically relevant solution we could consider blood, whose typical protein  
354 concentration can be estimated the following way. The most abundant proteins in blood are albumins  
355 (constituting about 55% of blood proteins), which are present in 3-5 g/dL concentration. The molar  
356 weight of albumins is around 65 kDalton (or 65000 g/mol). Taking 5 g/dL concentration this would  
357 yield a concentration of  $7.69 \cdot 10^{-4}$  M. Most other proteins present in blood have a much higher  
358 molecular weight (e.g. the molar mass of globulins is between 93-1193 kDalton), thus they increase  
359 only slightly the molar protein concentration of blood or they are present in much smaller quantities  
360 e.g. typical blood level of insulin between meals is  $57 \cdot 10^{-4}$  M.[43] This implies that blood is a  
361 slightly more diluted protein solution than the insulin solution studied by us, thus the 5 water layers  
362 is likely to be present around protein in blood and most likely in other physiologically relevant  
363 solutions. It is worth keeping in mind, though, that blood and other physiological solutions contain  
364 a variety of other co-solutes, e.g. sugars and other small molecules, which also influence the water  
365 network in them. Furthermore, from smaller peptides one may prepare much more concentrated  
366 solutions, where the individual peptide molecules may be closer to each other and there could be less  
367 than 8-10 hydration layers between two peptide molecules (i.e. 5 layers belonging to peptide 1 and  
368 five layers belonging to peptide would yield a separation of 10 layers). In this case it is very likely  
369 that proteins would seriously influence each other's solvation spheres, and in this case our  
370 conclusions would not be valid. A separate study would be needed to study the effect of peptide  
371 concentration on the structure of the hydration shells of peptides.

## 372 **Conclusions**

373 In this work we have studied the topological properties of the water layers around protein molecules  
374 as a function of sodium chloride concentration, using insulin as a model system. Our statistical  
375 analysis shows a significant difference among the hydrogen-bonded properties of water molecules  
376 in the first, second and farther solvation layers. We can also show that water molecules over the  
377 hydrophilic and hydrophobic surface of the protein possess slightly different H-bonding properties,  
378 supporting the hypothesis of structural and dynamical heterogeneity of the water molecules over the  
379 protein surface. The effect of the protein on the hydrogen bonded water network exist at least up to  
380 4 layers, which is in accordance with recently reported sub-terahertz spectroscopic measurements.

## 381 **Acknowledgements**

382 A.L. thanks the financial support for the Richter Gedeon Talentum Foundation. J.O. was supported  
383 by the Bolyai János Research Scholarship and by NKFIH Grant No. 115503. I.B. was supported by  
384 OTKA Grant No. 108721.

385

386 **References**

- 387 1 Frauenfelder H, Sligar SG & Wolynes PG (1991) The energy landscapes and motions of  
388 proteins. *Science* **254**, 1598–1603.
- 389 2 Austin RH, Beeson KW, Eisenstein L, Frauenfelder H & Gunsalus IC (1975) Dynamics of ligand  
390 binding to myoglobin. *Biochemistry* **14**, 5355–5373.
- 391 3 Hofmeister F (1888) On the understanding of the effect of salts. Second report. On regularities in  
392 the precipitating effect of salts and their relationship to their physiological behavior. *Naunyn-  
393 Schmiedebergs Arch. Exp. Pathol. Pharmacol* **24**, 247–260.
- 394 4 Baldwin RL (1996) How Hofmeister ion interactions affect protein stability. *Biophys. J.* **71**,  
395 2056–2063.
- 396 5 Bogár F, Bartha F, Násztor Z, Fábrián L, Leitgeb B & Dér A (2014) On the Hofmeister Effect:  
397 Fluctuations at the Protein–Water Interface and the Surface Tension. *J. Phys. Chem. B* **118**,  
398 8496–8504.
- 399 6 Bennion BJ & Daggett V (2003) The molecular basis for the chemical denaturation of proteins  
400 by urea. *Proc. Natl. Acad. Sci. U. S. A.* **100**, 5142–5147.
- 401 7 Otting G, Liepinsh E & Wüthrich K (1991) Protein hydration in aqueous solution. *Science* **254**,  
402 974–980.
- 403 8 Denisov VP & Halle B (1996) Protein hydration dynamics in aqueous solution. *Faraday Discuss.*  
404 **103**, 227–244.
- 405 9 Wiesner S, Kurian E, Prendergast FG & Halle B (1999) Water molecules in the binding cavity of  
406 intestinal fatty acid binding protein: dynamic characterization by Water17O and 2H magnetic  
407 relaxation dispersion. *J. Mol. Biol.* **286**, 233–246.
- 408 10 Henschman RH & McCammon JA (2002) Structural and dynamic properties of water around  
409 acetylcholinesterase. *Protein Sci.* **11**, 2080–2090.
- 410 11 Pal SK & Zewail AH (2004) Dynamics of water in biological recognition. *Chem. Rev.* **104**,  
411 2099–2123.
- 412 12 Russo D, Hura G & Head-Gordon T (2004) Hydration dynamics near a model protein surface.  
413 *Biophys. J.* **86**, 1852–1862.
- 414 13 Rosky PJ & Cheng Y-K (1998) Surface topography dependence of biomolecular hydrophobic  
415 hydration. *Nature* **392**, 696–699.
- 416 14 Makarov V, Pettitt BM & Feig M (2002) Solvation and hydration of proteins and nucleic acids:  
417 A theoretical view of simulation and experiment. *Acc. Chem. Res.* **35**, 376–384.
- 418 15 Makarov VA, Andrews BK, Smith PE & Pettitt BM (2000) Residence Times of Water  
419 Molecules in the Hydration Sites of Myoglobin. *Biophys. J.* **79**, 2966–2974.
- 420 16 Oleinikova A & Brovchenko I (2011) What Determines the Thermal Stability of the Hydrogen-  
421 Bonded Water Network Enveloping Peptides? *J. Phys. Chem. Lett.* **2**, 765–769.
- 422 17 Ebbinghaus S, Kim SJ, Heyden M, Yu X, Heugen U, Gruebele M, Leitner DM & Havenith M  
423 (2007) An extended dynamical hydration shell around proteins. *Proc. Natl. Acad. Sci.* **104**,  
424 20749–20752.

- 425 18 Sushko O, Dubrovka R & Donnan RS (2015) Sub-terahertz spectroscopy reveals that proteins  
426 influence the properties of water at greater distances than previously detected. *J. Chem. Phys.*  
427 **142**, 55101.
- 428 19 Wang C-H, Bai P, Siepmann JI & Clark AE (2014) Deconstructing Hydrogen-Bond Networks  
429 in Confined Nanoporous Materials: Implications for Alcohol–Water Separation. **118**, 19723–  
430 19732.
- 431 20 Choi J-H & Cho M (2014) Ion aggregation in high salt solutions. II. Spectral graph analysis of  
432 water hydrogen-bonding network and ion aggregate structures. *J. Chem. Phys.* **141**, 154502.
- 433 21 Lee H, Choi J-H, Verma PK & Cho M (2015) Spectral Graph Analyses of Water Hydrogen-  
434 Bonding Network and Osmolyte Aggregate Structures in Osmolyte-Water Solutions. *J. Phys.*  
435 *Chem. B* **119**, 14402–14412.
- 436 22 Bakó I, Oláh J, Lábás A, Bálint S, Pusztai L & Bellissent Funel MC (2017) Water-formamide  
437 mixtures: Topology of the hydrogen-bonded network. *J. Mol. Liq.* **228**, 25–31.
- 438 23 Bakó I, Bencsura Á, Hermansson K, Bálint S, Grósz T, Chihaiia V & Oláh J (2013) Hydrogen  
439 bond network topology in liquid water and methanol: a graph theory approach. *Phys. Chem.*  
440 *Chem. Phys.* **15**, 15163–15171.
- 441 24 Mezei M (2003) A new method for mapping macromolecular topography. *J. Mol. Graph.*  
442 *Model.* **21**, 463–472.
- 443 25 Willard AP & Chandler D (2010) Instantaneous Liquid Interfaces. *J. Phys. Chem. B* **114**, 1954–  
444 1958.
- 445 26 Sega M, Kantorovich SS, Jedlovsky P & Jorge M (2013) The generalized identification of  
446 truly interfacial molecules (ITIM) algorithm for nonplanar interfaces. *J. Chem. Phys.* **138**,  
447 44110.
- 448 27 Timofeev V., Chuprov-Netochin R., Samigina V., Bezuglov V., Miroshnikov K. & Kuranova IP  
449 (2010) X-ray investigation of gene-engineered human insulin crystallized from a solution  
450 containing polysialic acid. *Acta Crystallogr., Sect. F* **66**, 259–263.
- 451 28 Anandkrishnan R, Aguilar B & Onufriev A V (2012) H++ 3.0: automating pK prediction and  
452 the preparation of biomolecular structures for atomistic molecular modeling and simulations.  
453 *Nucleic Acids Res.* **40**, W537-541.
- 454 29 Myers J, Grothaus G, Narayanan S & Onufriev A (2006) A simple clustering algorithm can be  
455 accurate enough for use in calculations of pKs in macromolecules. *Proteins* **63**, 928–938.
- 456 30 Gordon JC, Myers JB, Folta T, Shoja V, Heath LS & Onufriev A (2005) H++: a server for  
457 estimating pKas and adding missing hydrogens to macromolecules. *Nucleic Acids Res.* **33**,  
458 W368-371.
- 459 31 Jo S, Kim T, Iyer VG & Im W (2008) CHARMM-GUI: a web-based graphical user interface  
460 for CHARMM. *J. Comput. Chem.* **29**, 1859–1865.
- 461 32 Phillips JC, Braun R, Wang W, Gumbart J, Tajkhorshid E, Villa E, Chipot C, Skeel RD, Kalé L  
462 & Schulten K (2005) Scalable molecular dynamics with NAMD. *J. Comput. Chem.* **26**, 1781–  
463 1802.
- 464 33 MacKerell AD, Banavali N & Foloppe N (2000) Development and current status of the  
465 CHARMM force field for nucleic acids. *Biopolymers* **56**, 257–265.
- 466 34 Brooks BR, Brooks CL, Mackerell AD, Nilsson L, Petrella RJ, Roux B, Won Y, Archontis G,



- 467 Bartels C, Boresch S, Caflisch A, Caves L, Cui Q, Dinner AR, Feig M, Fischer S, Gao J,  
468 Hodosek M, Im W, Kuczera K, Lazaridis T, Ma J, Ovchinnikov V, Paci E, Pastor RW, Post  
469 CB, Pu JZ, Schaefer M, Tidor B, Venable RM, Woodcock HL, Wu X, Yang W, York DM &  
470 Karplus M (2009) CHARMM: the biomolecular simulation program. *J. Comput. Chem.* **30**,  
471 1545–1614.
- 472 35 Ryckaert J-P, Ciccotti G & Berendsen HJ. (1977) Numerical integration of the cartesian  
473 equations of motion of a system with constraints: molecular dynamics of n-alkanes. *J.*  
474 *Comput. Phys.* **23**, 327–341.
- 475 36 De Loof H, Nilsson L & Rigler R (1992) Molecular dynamics simulation of galanin in aqueous  
476 and nonaqueous solution. *J. Am. Chem. Soc.* **114**, 4028–4035.
- 477 37 Wendler K, Thar J, Zahn S & Kirchner B (2010) Estimating the Hydrogen Bond Energy. *J.*  
478 *Phys. Chem. A* **114**, 9529–9536.
- 479 38 Nayar D & Chakravarty C (2014) Sensitivity of local hydration behaviour and conformational  
480 preferences of peptides to choice of water model. *Phys. Chem. Chem. Phys.* **16**, 10199–10213.
- 481 39 Rani P & Biswas P (2014) Shape dependence of the radial distribution function of hydration  
482 water around proteins. *J. Phys. Condens. Matter* **26**, 335102.
- 483 40 Rani P & Biswas P (2015) Local Structure and Dynamics of Hydration Water in Intrinsically  
484 Disordered Proteins. *J. Phys. Chem. B* **119**, 10858–10867.
- 485 41 Abhishek Rastogi AKG and SJS (2011) *Hydrogen bond interactions between water molecules*  
486 *in bulk liquid, near electrode surfaces and around ions* InTech.
- 487 42 Oleinikova A, Brovchenko I, Smolin N, Krukau A, Geiger A & Winter R (2005) Percolation  
488 Transition of Hydration Water: From Planar Hydrophilic Surfaces to Proteins. *Phys. Rev. Lett.*  
489 **95**, 247802.
- 490 43 Iwase H, Kobayashi M, Nakajima M, Takatori T, Rindfrey H, Lang H, Leybold K, Rick W &  
491 Staudinger HJ (2001) The ratio of insulin to C-peptide can be used to make a forensic  
492 diagnosis of exogenous insulin overdose. *Forensic Sci. Int.* **115**, 123–127.
- 493

494

495 **Table 1. Average protein RMSD values calculated for backbone heavy atoms in Å in the**  
496 **three parallel 5 ns long MD simulations with their standard deviations for all systems.**

Chain	Structure	Neutral	0.5 M	1.5 M
A	Helices	<b>1.72 ± 0.97</b>	<b>1.74 ± 1.20</b>	<b>1.44 ± 1.07</b>
A	Turn	<b>1.56 ± 0.24</b>	<b>1.69 ± 0.45</b>	<b>1.28 ± 0.28</b>
A	Loop	<b>3.67 ± 3.42</b>	<b>2.98 ± 1.77</b>	<b>2.32 ± 1.54</b>
B	Helix	<b>1.87 ± 0.87</b>	<b>1.96 ± 0.89</b>	<b>1.66 ± 0.79</b>
B	Loops	<b>1.87 ± 0.80</b>	<b>2.00 ± 0.79</b>	<b>1.53 ± 0.91</b>

497

498

499

500

501

502 **Table 2. Number of water molecules in shells with their standard deviations around the**  
 503 **protein averaged over all snapshots and three parallel MD simulations and total number of**  
 504 **water molecules/ions in the simulation box as a function of salt concentrations**

<b>Water layer</b>	<b>Neutral</b>	<b>0.5 M</b>	<b>1.5 M</b>
<b>1</b>	<b>269 ±3</b>	<b>269 ±4</b>	<b>263 ±4</b>
<b>1</b> <i>hydrophobic</i>	<b>149 ±3</b>	<b>150 ±3</b>	<b>150 ±2</b>
<b>1</b> <i>hydrophilic</i>	<b>120 ±1</b>	<b>119 ±3</b>	<b>113 ±2</b>
<b>2</b>	<b>297± 4</b>	<b>296 ±4</b>	<b>287 ±3</b>
<b>3</b>	<b>389 ±4</b>	<b>386 ±5</b>	<b>374 ±3</b>
<b>4</b>	<b>493 ±5</b>	<b>490± 5</b>	<b>478 ±4</b>
<b>5</b>	<b>611 ±5</b>	<b>607 ±4</b>	<b>594 ±5</b>
<b>N<sub>water</sub></b>	<b>6445</b>	<b>6104</b>	<b>5459</b>
<b>N<sub>sodium</sub></b>	<b>1</b>	<b>61</b>	<b>182</b>
<b>N<sub>chloride</sub></b>	<b>0</b>	<b>60</b>	<b>181</b>
<b>N<sub>water, reference</sub></b>	<b>6657</b>	<b>6397</b>	<b>5800</b>

505

506

507

508 **Table 3. The average number of hydrogen bonds with their standard deviations formed**  
 509 **between protein and 1<sup>st</sup> solvation layer, and between the rest of the solvation shells at**  
 510 **different salt concentrations. Data is averaged over the three parallel MD simulations and**  
 511 **over all snapshots. “All” denotes the sum of all hydrogen bonds towards any partner.**  
 512 **Solvation layers are designated by numbers.**

<b>Hydrogen bond partners</b>	<b>Neutral</b>	<b>0.5 M</b>	<b>1.5 M</b>
<b>1<sup>st</sup> - 1<sup>st</sup></b>	<b>1.84 ± 0.01</b>	<b>1.81 ± 0.01</b>	<b>1.76 ± 0.00</b>
<b>1<sup>st</sup> - protein</b>	<b>0.56 ± 0.02</b>	<b>0.55 ± 0.02</b>	<b>0.55 ± 0.01</b>
<b>1<sup>st</sup> - protein<sup>hydrophilic</sup></b>	<b>1.25 ± 0.04</b>	<b>1.26 ± 0.06</b>	<b>1.26 ± 0.03</b>
<b>1<sup>st</sup> - all water</b>	<b>3.05 ± 0.02</b>	<b>2.98 ± 0.01</b>	<b>2.84 ± 0.03</b>
<b>1<sup>st,hydrophilic</sup> - all water</b>	<b>2.54 ± 0.02</b>	<b>2.49 ± 0.02</b>	<b>2.36 ± 0.02</b>
<b>1<sup>st,hydrophobic</sup> - all water</b>	<b>3.46 ± 0.01</b>	<b>3.37 ± 0.02</b>	<b>3.18 ± 0.02</b>
<b>1<sup>st</sup> – all (protein+ water)</b>	<b>3.61 ± 0.02</b>	<b>3.53 ± 0.01</b>	<b>3.39 ± 0.02</b>
<b>2<sup>nd</sup> - 2<sup>nd</sup></b>	<b>1.18 ± 0.01</b>	<b>1.14 ± 0.01</b>	<b>1.06 ± 0.01</b>
<b>2<sup>nd</sup> - all water</b>	<b>2.91 ± 0.01</b>	<b>2.79 ± 0.02</b>	<b>2.57 ± 0.02</b>
<b>3<sup>rd</sup> - 3<sup>rd</sup></b>	<b>1.17 ± 0.01</b>	<b>1.13 ± 0.01</b>	<b>1.04 ± 0.01</b>
<b>3<sup>rd</sup> – all water</b>	<b>3.69 ± 0.01</b>	<b>3.56 ± 0.04</b>	<b>3.28 ± 0.03</b>
<b>4<sup>th</sup> - 4<sup>th</sup></b>	<b>1.17 ± 0.01</b>	<b>1.13 ± 0.01</b>	<b>1.04 ± 0.01</b>
<b>4<sup>th</sup> – all water</b>	<b>3.68 ± 0.03</b>	<b>3.54 ± 0.05</b>	<b>3.26 ± 0.05</b>
<b>reference systems</b>	<b>3.40 ± 0.01</b>	<b>3.40 ± 0.01</b>	<b>3.14 ± 0.01</b>

513

514

515 **Table 4. The average number of hydrogen bonds using various C...O distance criteria for**  
516 **identifying hydrophobic water molecules in the first hydration shell in protein simulations at**  
517 **0.5 M NaCl concentration. “All” denotes the sum of all hydrogen bonds towards any partner.**  
518 **Solvation layers are designated by numbers.**

<b>Hydrogen bond partners</b>	<b>5.00 Å</b>	<b>4.50 Å</b>	<b>4.25 Å</b>	<b>4.00 Å</b>
<b>1<sup>st</sup> - all water</b>	3.07	2.99	2.93	2.85
<b>2<sup>nd</sup> - all water</b>	2.82	2.80	2.79	2.77
<b>3<sup>rd</sup> - all water</b>	3.58	3.58	3.58	3.58
<b>4<sup>th</sup> - all water</b>	3.57	3.57	3.57	3.57

519

520

521 **Table 5. The average number of hydrogen bonds at 0.5 M NaCl concentration calculated**  
 522 **using various angle criteria for defining a hydrogen bond. “All” denotes the sum of all**  
 523 **hydrogen bonds towards any partner. Solvation layers are designated by numbers.**

<b>Hydrogen bond partners</b>	<b>120°</b>	<b>130°</b>	<b>145°</b>
<b>1st - 1st</b>	1.63	1.54	1.27
<b>1st - all water</b>	2.93	2.77	2.27
<b>2<sup>nd</sup> - 2<sup>nd</sup></b>	1.14	1.07	0.85
<b>2<sup>nd</sup> - all water</b>	2.54	2.38	1.92
<b>3<sup>rd</sup> - 3<sup>rd</sup></b>	1.13	1.06	0.84
<b>3<sup>rd</sup> - all water</b>	3.58	3.36	2.72
<b>4<sup>th</sup> - 4<sup>th</sup></b>	1.14	1.06	0.85
<b>4<sup>th</sup> - all water</b>	3.57	3.36	2.72

524

525

526 **Table 6. The average energy (kJ/mol) of hydrogen bonds with their standard deviations**  
 527 **formed between molecules within the same layer and between molecules in neighboring**  
 528 **layers.**

	<b>Neutral</b>	<b>0.5 M</b>	<b>1.5 M</b>
<b>1<sup>st</sup> - 1<sup>st</sup></b>	<b>-15.73 ± 0.02</b>	<b>-15.68 ± 0.01</b>	<b>-15.63 ± 0.03</b>
<b>1<sup>st</sup>,hydrophilic - 1<sup>st</sup>,hydrophilic</b>	<b>-15.07 ± 0.04</b>	<b>-14.96 ± 0.03</b>	<b>-14.91 ± 0.04</b>
<b>1<sup>st</sup>,hydrophobic - 1<sup>st</sup>,hydrophobic</b>	<b>-15.78 ± 0.04</b>	<b>-15.70 ± 0.04</b>	<b>-15.53 ± 0.04</b>
<b>1<sup>st</sup> - 2<sup>nd</sup></b>	<b>-15.14 ± 0.02</b>	<b>-15.03 ± 0.01</b>	<b>-14.83 ± 0.03</b>
<b>2<sup>nd</sup> - 2<sup>nd</sup></b>	<b>-14.95 ± 0.01</b>	<b>-14.87 ± 0.01</b>	<b>-14.68 ± 0.02</b>
<b>2<sup>nd</sup> - 3<sup>rd</sup></b>	<b>-15.49 ± 0.01</b>	<b>-15.34 ± 0.01</b>	<b>-15.05 ± 0.03</b>
<b>3<sup>rd</sup> - 3<sup>rd</sup></b>	<b>-15.01 ± 0.02</b>	<b>-14.88 ± 0.01</b>	<b>-14.65 ± 0.01</b>
<b>3<sup>rd</sup> - 4<sup>th</sup></b>	<b>-15.50 ± 0.01</b>	<b>-15.34 ± 0.01</b>	<b>-15.03 ± 0.02</b>
<b>4<sup>th</sup> - 4<sup>th</sup></b>	<b>-15.20 ± 0.02</b>	<b>-14.98 ± 0.01</b>	<b>-14.65 ± 0.01</b>
<b>4<sup>th</sup> - 5<sup>th</sup></b>	<b>-15.51 ± 0.01</b>	<b>-15.35 ± 0.01</b>	<b>-15.01 ± 0.01</b>
<b>Reference systems</b>	<b>-15.91 ± 0.01</b>	<b>-15.67 ± 0.01</b>	<b>-15.55 ± 0.01</b>

529

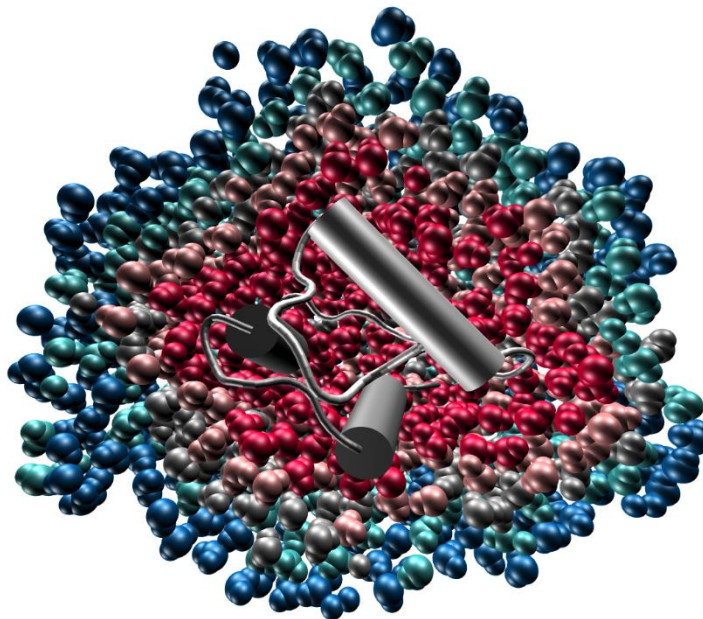
530

531 **Table 7. The average energy (kJ/mol) of hydrogen bonds at 0.5 M NaCl concentration**  
 532 **calculated using various angle criteria for defining a hydrogen bond. Solvation layers are**  
 533 **designated by numbers.**

	120°	130°	145°
1 <sup>st</sup> - 1 <sup>st</sup>	-15.66	-16.79	-18.21
1 <sup>st</sup> - 2 <sup>nd</sup>	-15.11	-16.04	-17.42
2 <sup>nd</sup> - 2 <sup>nd</sup>	-14.86	-16.08	-17.58
2 <sup>nd</sup> - 3 <sup>rd</sup>	-15.32	-16.20	-17.54
3 <sup>rd</sup> - 3 <sup>rd</sup>	-14.86	-16.12	-17.58
3 <sup>rd</sup> - 4 <sup>th</sup>	-15.32	-16.20	-17.50
4 <sup>th</sup> - 4 <sup>th</sup>	-15.16	-16.08	-17.33
4 <sup>th</sup> - 5 <sup>th</sup>	-15.37	-16.08	-17.25
5 <sup>th</sup> - 5 <sup>th</sup>	-14.91	-15.66	-16.87

534  
 535



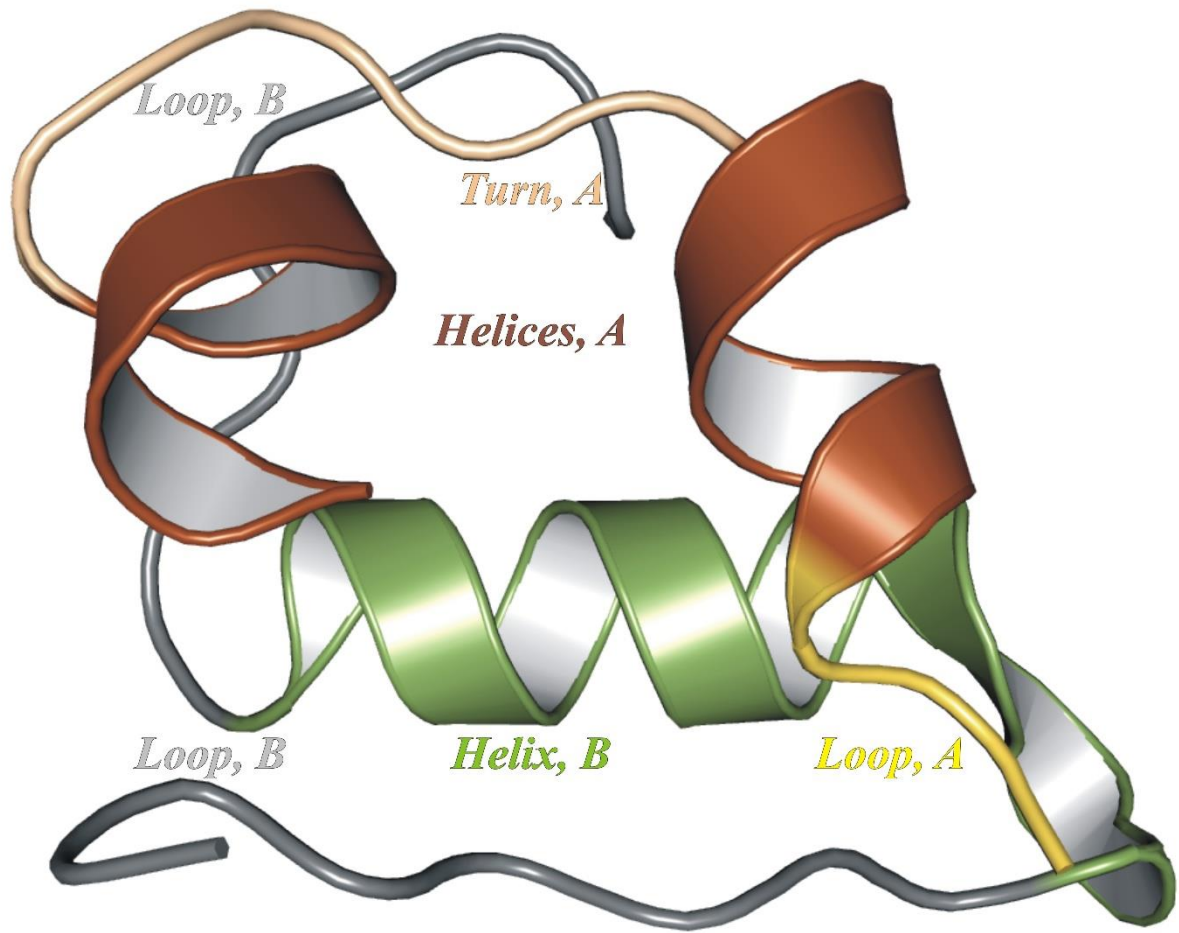


536

537

**Figure 1. Schematic representation of the hydration sphere layers around the protein.**

538



539

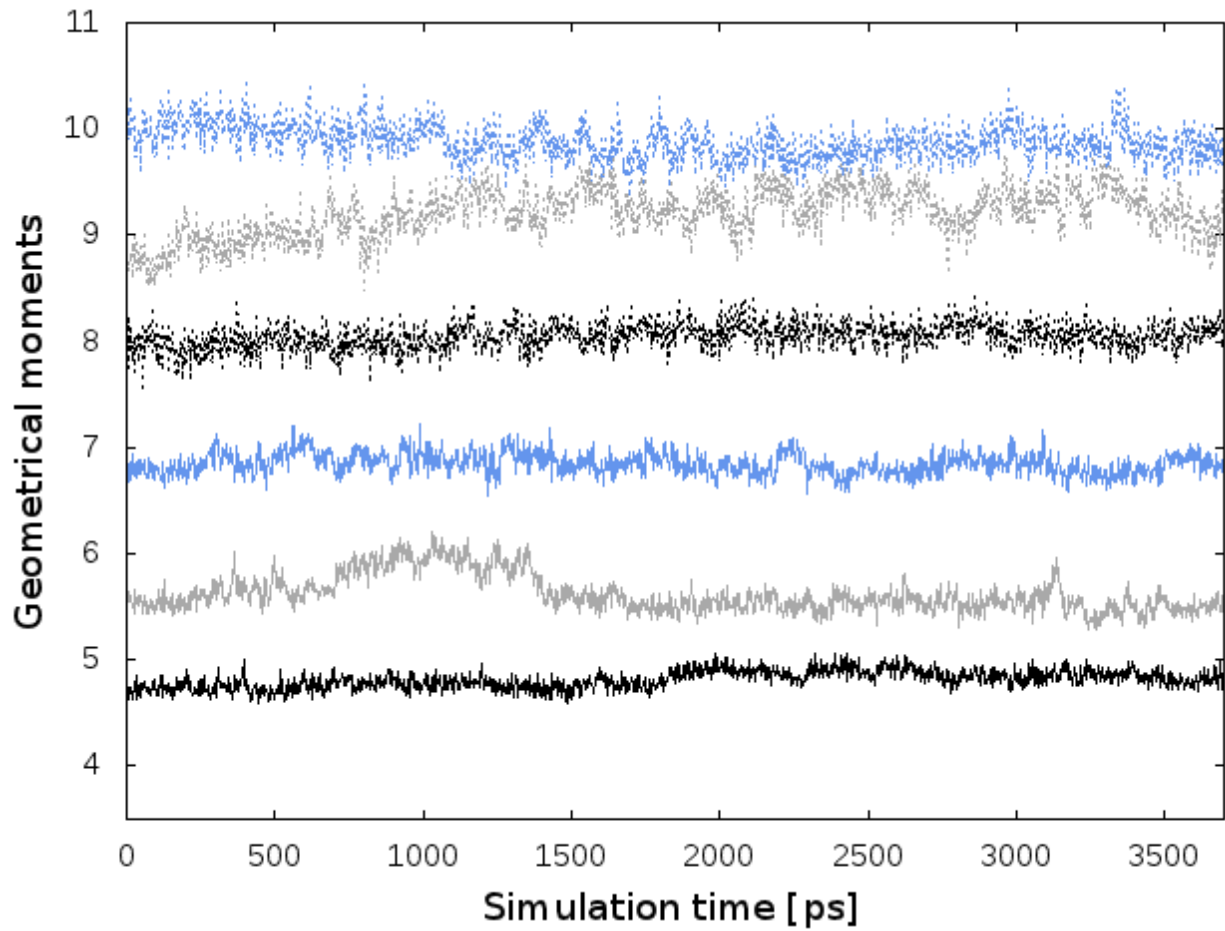
540

541

542

543

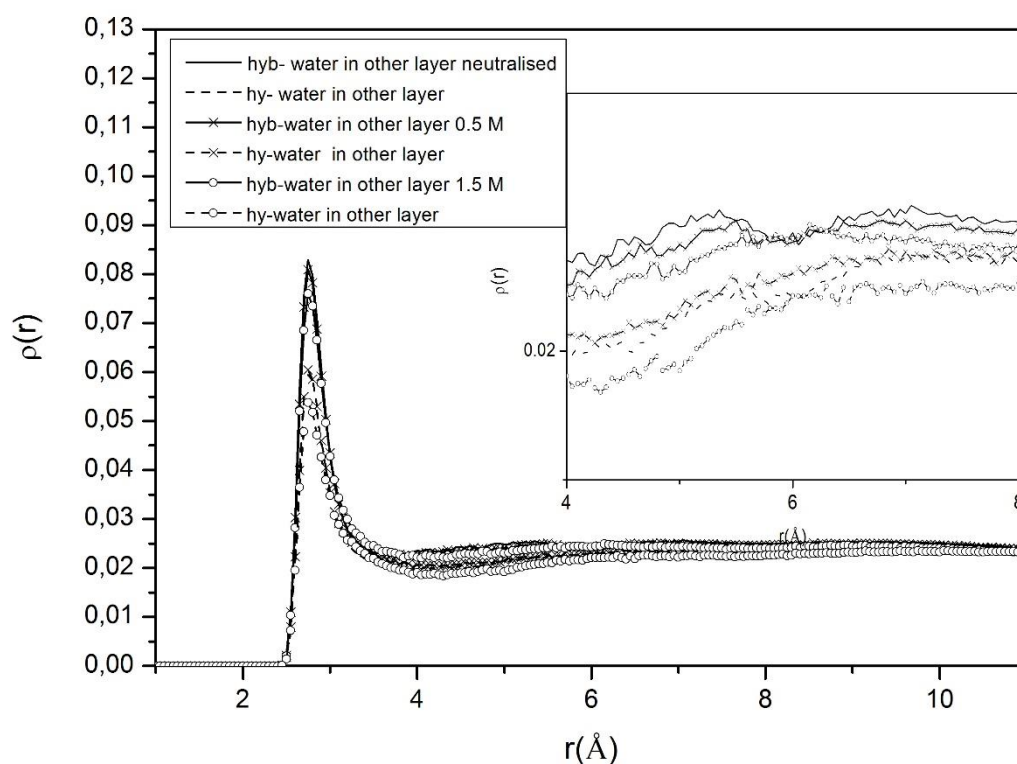
**Figure 2. Structural elements in the insulin monomer.** Colors used to depict the various structural elements in chain A : brown – helices; wheat – turn; yellow – loop; while in chain B: green – helix; grey – loops.



544

545 **Figure 3. The inertia moments during the simulations.** Inercia momemnts belong to protein  
 546 shown with lines. Data include the protein and the first three water layers are represented with  
 547 dotted lines. The three moment components are shown in black, gray and ice blue.

548



549

550

551

552

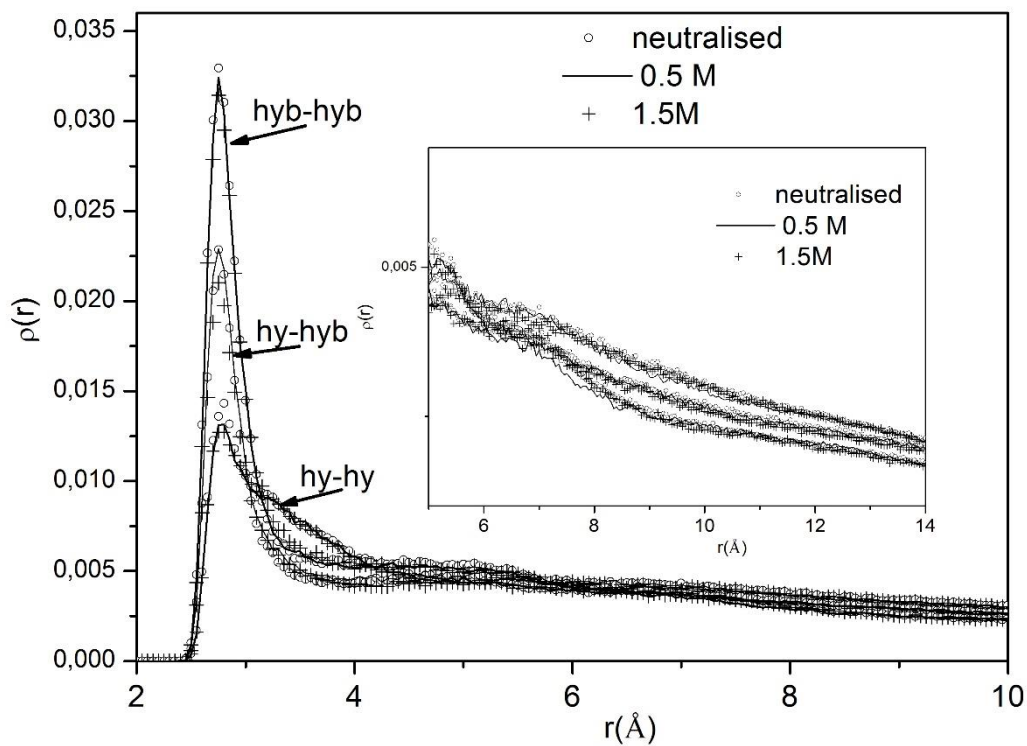
553

554

555

556

**Figure 4. Decomposition of the raw density distribution function (of-the  $O_{\text{water}}-O_{\text{water}}$  distance) of water molecules in the first hydration layer interacting with water molecules in outer layers according to the hydrophilic (it forms H-bonds with the protein) or hydrophobic (it forms no H-bonds with the protein) nature of the water molecules in the first solvation layer at various salt concentrations.**



557

558 **Figure 5 Decomposition of the raw density distribution function (of-the  $O_{\text{water}}-O_{\text{water}}$  distance)**  
 559 **among water molecule in the first hydration shell according to the nature of interacting**  
 560 **water molecules: Hydrophobic water: it forms no H-bonds with the protein, hydrophylic**  
 561 **water: it forms H-bonds with the protein at various salt concentrations.**